Acta Crystallographica Section D
Biological Crystallography
ISSN 0907-4449

Crystallization and preliminary X-ray diffraction analysis of two homologous antigen-binding fragments in complex with different carbohydrate antigens

Hoa P. Nguyen,[a]* Nina O. L. Seto,[b] Lore Brade,[c] Paul Kosma,[d] Helmut Brade[c] and Stephen V. Evans[a]

[a]Department of Biochemistry, Microbiology and Immunology, University of Ottawa, 451 Smyth Road, Ottawa, Ontario K1H 8M5, Canada, [b]Institute of Biological Sciences, National Research Council, 100 Sussex Drive, Ottawa, Ontario K1A 0R6, Canada, [c]Division of Medical and Biochemical Microbiology, Research Center Borstel, Center for Medicine and Biosciences, D-23845 Borstel, Germany, and [d]Institute of Chemistry, University of Agriculture, A-1190 Vienna, Austria

Correspondence e-mail: evans@uottawa.ca

Received 19 April 2001
Accepted 6 September 2001

The antigen-binding fragments (Fab) of two murine monoclonal antibodies (mAb) S25-2 and S45-18, specific for carbohydrate epitopes in the lipopolysaccharide of the bacterial family *Chlamydiaceae*, have been crystallized in the presence and absence of synthetic oligosaccharides corresponding to their respective haptens. Crystals of both Fabs show different morphology depending on the presence of antigens. The sequence of mAb S45-18 was determined and shows a remarkable homology to that reported for mAb S25-2. These crystals offer an unparalleled opportunity to compare the structure and modes of binding of two homologous antibodies to similar but distinct carbohydrate epitopes.

1. Introduction

Anticarbohydrate antibodies are known to be able to distinguish between closely related antigens, but there are too few reported structures of antibodies in complex with their carbohydrate antigens to fully understand the structural basis for their recognition. One common feature of anticarbohydrate antibodies appears to be their relatively low binding affinities for antigen, which are typically 10^4 times weaker than the interactions of antiprotein or antipeptide antibodies with their antigen. This single observation may explain why there are relatively few structures reported of anticarbohydrate antibodies in complex with antigen. Known structures include Se155-4 with *Salmonella* bacterial membrane oligosaccharides (Zdanov *et al.*, 1994; Bundle *et al.*, 1994; Cygler *et al.*, 1991), the antitumour BR96 (Jeffrey *et al.*, 1995) and recently S20-4, also with bacterial saccharides (Villeneuve *et al.*, 2000).

The best known example of antibody recognition of carbohydrate antigens lies in the human ABO blood-group antigens. The only difference between the A and B trisaccharide antigens is the substitution of one *N*-acetyl group for one hydroxyl group, yet the recognition by host antibodies of either antigen on the red blood cells of a mismatched transfusion can have catastrophic consequences (Capon & Goldfinger, 1995). However significant, the human ABO blood group only provides one pair of antibody–antigen interactions. A much larger panel of potential interactions can be found in studying members of the bacterial family *Chlamydiaceae*. An intriguing surface component that is recognized during infection is the genus-specific lipopolysaccharide (LPS), which is believed to play roles in host-cell invasion, disruption of intracellular phagolysosome fusion and disruption of cellular trafficking (Kosma, 1999; Ryan, 1994). *Chlamydia trachomatis* is the leading cause of bacterially transmitted sexual infection. Salpingitis, pelvic inflammatory disease and infertility are among the many serious sequelae of infection (Ryan, 1994). *Trachomatis* ocular infection also accounts for a high prevelance of preventable secondary blindness, particularly in underdeveloped countries. *C. pneumoniae* causes lower respiratory tract infection and is of concern in immunodepressed patients. Its role in the promotion of atherosclerosis has also been of recent debate (Kalayoglu *et al.*, 2000). *C. psittaci* infection is often transferred from infected animals and may also result in serious complications (Ryan, 1994).

Antibodies have been produced against a large number of these chlamydial LPS epitopes, which differ both in the chemical identity and linkage of the monosaccharide units composed of 3-deoxy-D-*manno*-oct-2-ulosonic acid (Kdo) (Brade, Brade *et al.*, 1987; Brade, Kosma *et al.*, 1987). Two murine mAb $IgG_{1\kappa}$s in particular, S25-2 and S45-18, offer insights into the phenomenon of antibody–carbohydrate binding. S25-2 displays a preferential binding to the unique terminal genus-specific α-2,8 linkage (Müller-Loennies *et al.*, 2000; Brade, Brade *et al.*, 1987) formed by the chlamydial Kdo glycosyltransferase gseA (Holst *et al.*, 1995; Belunis *et al.*, 1992). Speci-

fically, S25-2 binds the α-Kdo-(2,8)-α-Kdo disaccharide and the trisaccharide α-Kdo-(2,8)-α-Kdo-(2,4)-α-Kdo with equal affinity and the terminal α-2,4-linked Kdo that is common in LPS of other Gram-negative bacteria with reduced affinity (Müller-Loennies *et al.*, 2000). In contrast, while S45-18 is not selective for the α-2,8 linkage, it recognizes the terminal α-2,4 linkage. S45-18 has a binding preference for the trisaccharide epitope α-Kdo-(2,4)-α-Kdo-(2,4)-α-Kdo (Brade *et al.*, 2000).

The observation that the epitopes of S25-2 and S45-18 overlap provides a critical opportunity to compare how these different antibodies select for the same monosaccharides in different chemical contexts. The determination of the structures of these Fabs in complex with their carbohydrate antigen will add significantly to the understanding of protein–carbohydrate recognition. The amino-acid sequence of S25-2 has been reported previously (Müller-Loennies *et al.*, 2000). Here, we report the sequence of S45-18 and the crystallization and preliminary X-ray diffraction analysis of Fabs from S25-2 and S45-18 in their liganded and unliganded states.

2. Experimental

2.1. Generation of antibodies

Synthetic Kdo-BSA glycoconjugates shown to mimic the native binding of chlamydial Kdo (Fu *et al.*, 1992; Brade, Kosma *et al.*, 1987) have been used in the generation of the monoclonal murine $IgG_{1\kappa}$ S25-2 and S45-18, as previously described (Fu *et al.*, 1992).

2.2. Cloning of S45-18 variable domain genes

Hybridoma cells (5×10^6 cells) of S45-18 were pelleted by centrifugation at 1000*g* for 5 min at 277 K and washed with 10 ml of cold PBS solution. All general molecular biology procedures were performed according to standard protocols (Sambrook *et al.*, 1989). The total mRNA was isolated from the hybridoma cells according the to protocol for the Oligotex Direct mRNA isolation system (Qiagen Inc.) and the cell lysates were homogenized using a QIAshredder (Qiagen Inc.) and the purified mRNA was eluted in 70 µl of elution buffer at 343 K.

The S45-18 V_H gene was amplified by a one-step RT-PCR reaction as described for the Titan One Tube RT-PCR system (Boehringer Mannheim) using 5 µl of mRNA and the degenerate PCR primers MH-Fr1 (5′-TATATCCGGASAGGTNMA-RCTNSWGSAGTC-3′) and mC-IgG1+2B (5′-GAGAAGCTTTGGATAGACWGAT-GGGGGTGT-3′).

RT-PCR for amplification of the V_H gene was performed at 323 K for 30 s and 367 K for 3 min, followed by 30 cycles of 367 K for 30 s, 313 K for 1 min, 345 K for 45 s and completed with a final extension step of 10 min at 367 K. The PCR products were separated on 1% agarose gels by electrophoresis, purified with the QIAquick PCR purification system (Qiagen Inc.) and eluted in a 30 µl total volume. The purified DNA from the RT-PCR was amplified by using 10 µl of the first RT-PCR product as a template using the same primers in a standard PCR reaction at 367 K for 3 min followed by 30 cycles of 367 K for 30 s, 327 K for 30 s, 345 K for 60 s and completed with a final extension step of 10 min at 394 K (Erlich, 1989).

The S45-18 V_L gene was amplified by RT-PCR using 8 µl of mRNA and the PCR primers NLB15 (5′-CCGCCGCCGCGTG-CACTCGAYATTGTGATGACCCAGWT-3′) and mC-κ (5′-GAGAAGCTTTGGGAA GATGGATACAGTTGG-3′) as follows: 323 K for 30 s, 367 K for 3 min, followed by 30 cycles of 367 K for 30 s, 323 K for 1 min, 367 K for 45 s and completed with a final extension at 367 K for 10 min. The RT-PCR reaction was sufficient for the amplification of the V_L gene. The amplified V_L gene was purified as described above and digested with the restriction enzyme *Pfl*MI (New England Biolabs) to remove any endogenous aberrant κ chains which might have co-amplified with the S45-18 V_L gene. There was no digestion of the PCR product, which shows that the commonly amplified endogenous aberrant κ chains were not present in this PCR reaction (Duan & Pomerantz, 1994).

The PCR products containing the V_H and V_L genes were cloned using the pGEM-T-Easy system (Promega Corp.). Plasmid DNA was purified using the QIAprep Miniprep system (Qiagen Inc.) and the DNA sequence of the genes were determined using an Applied Biosystems 373 automated system. The antibody S45-18 was isolated from the culture supernatant of the hybridoma cell line and the N-terminal

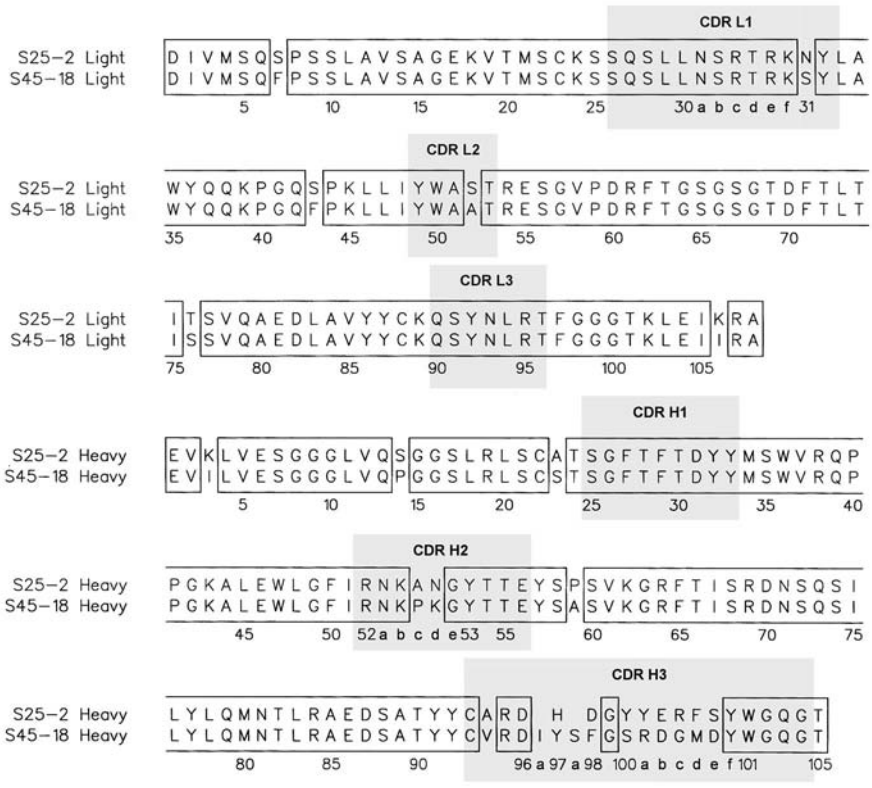

Figure 1
Alignment of the amino-acid sequence of the variable domains of the two murine mAb $IgG_{1\kappa}$s S25-2 and S45-18, using the one-letter abbreviation. The defined locations of the six hypervariable CDRs (Al-Lazikani *et al.*, 1997; Chothia *et al.*, 1989; Kabat, 1988) are shaded. Most of the sequence variation between S25-2 and S45-18 occurs in the third CDR of the heavy chain, where there are two amino-acid insertions in the sequence of S45-18.

amino-acid sequence of its chains was determined to confirm that the correct genes have been cloned.

2.3. Analysis of the variable-domain sequences

The amplification and cloning of murine hybridoma-specific immunoglobulin genes using pooled degenerate-primer polymerase chain reaction technology (PCR) is based on the conserved 5′ terminus of the immunoglobulin gene variable regions and the constant regions in the 3′ terminus (Borrebaeck, 1992).

The genes encoding the two variable domains of S45-18 were amplified by PCR and the DNA sequence was determined. Pools of degenerate PCR primers which annealed to the partly conserved regions at both ends of the variable-domain sequences were used for this purpose. For both V_H and V_L, only one amplification product was found. The correct amplification of the antibody S45-18 was confirmed by isolating the antibody from the culture supernatant of the hybridoma cell line and performing N-terminal amino-acid sequence analysis of its chains. The first 21 amino acids of V_L corresponded to the amplified cDNA. The first 22 amino acids of V_H also corresponded to the cloned DNA sequence except for amino acid 19 (cannot be affected by the PCR primers used for amplification), which was Arg in the DNA and Lys in the amino-acid sequence.

Alignment of the S45-18 variable domain amino-acid sequence with that of S25-2 (Müller-Loennies *et al.*, 2000) reveals high sequence identity (Fig. 1). Based on reviews of canonical structures (Al-Lazikani *et al.*, 1997; Chothia *et al.*, 1989; Kabat, 1988), we predict the complementarity-determining regions (CDRs) that form the combining site of the two antibodies. These regions are highly conserved across both antibodies, with the exception of the third region of the variable heavy domain.

2.4. Preparation of Fab

S45-18 $IgG_{1\kappa}$ was purified from ascites fluid using a protein A affinity column chromatography (Protein A Affi-Gel from Bio-Rad, improved for subclass G1 binding). S25-2 was purified using a protein G affinity column (Protein G Sepharose 4FF from Pharmacia). The Fab are generated by papain digest (Papaya Latex mercuripapain from Sigma), using 1:100(*w*/*w*) papain:IgG, 2 m*M* EDTA, 5 m*M* dithiothreitol and 50 m*M* Tris–HCl pH 8.5, brought to final volume with 20 m*M* NaOAc pH 5.4. The final concentration of antibody in the reaction mixture is less than 1 mg ml^{-1}. SDS–PAGE was used to optimize digestion times. The reaction was quenched with 10 m*M* iodoacetamide after 4.5 h for S25-2 digest and after 3 h for S45-18 digest. The solution was dialyzed overnight at 277 K with two changes of 20 m*M* NaOAc buffer pH 5.4, filtered through a low protein binding 0.22 µm filter (Millipore) and degassed before proceeding with HPLC cation-exchange purification (Gilson Series 800 HPLC system, Gilson Scientific Canada, Inc.; Shodex CM-825 from Phenomenex). Digest volumes less than 1 ml were injected with a mobile phase of 20 m*M* Tris pH 9.1 flowing at 1 ml min^{-1}. Both the S25-2 Fab and the S45-18 Fab eluted in a 20-minute linear gradient of 0–1.2 *M* KCl, with corresponding Fab peaks appearing at about 1.0 *M* KCl. Samples were concentrated to 30 mg ml^{-1} using Centricon YM-10 centrifugal filter devices (Millipore) with a wash buffer of 20 m*M* Tris pH 9.1.

2.5. Crystallization trials

Crystallization conditions for the hanging-drop vapour-diffusion method were initially refined from Hampton Crystal Screen I conditions (Hampton Research). Optimized crystallization conditions are presented in Table 1.

2.5.1. Crystallization of unliganded Fab. Drops were mixed and suspended from plastic coverslips over 24-well Linbro tissue-culture plates (Flow Labs) sealed with silicone high-vacuum grease (Dow Corning) and from plastic covers of culture dishes (Corning) sealed with parafilm. Unliganded S25-2 Fab crystals were grown in drops of up to 4 µl suspended over 1 ml of reservoir solution. Precipitation was present upon inspection of the hanging drop. Crystals appeared after three weeks at 295 K. Microcrystals having a hexagonal face were commonly observed and most were non-monolithic (Fig. 3*a*). The crystal sizes did not exceed 0.25 × 0.15 × 0.1 mm after two months of observation and often fractured upon contact. Unliganded S45-18 Fab crystals grew from drops ranging in volume from 6 to 10 µl over a 1 ml reservoir. The drops were clear. Hexagonal plate and trapezoid-face rectangular crystals (Fig. 3*c*) appeared within a week at room temperature, after which crystals were transferred to 277 K. After about two weeks, single crystals with dimensions up to 0.6 × 0.4 × 0.3 mm were mounted in glass capillaries (Charles Supper Co.) for room-temperature diffraction.

2.5.2. Crystallization of Fab–carbohydrate complexes. For complexation trials of S25-2 and S45-18, the respective acid-labile α-Kdo-(2,8)-α-Kdo-2-*O*-allyl and α-Kdo-(2,4)-α-Kdo-(2,4)-α-Kdo-(2,6)-β-GlcN-4P-(1,6)-α-GlcN-1P pentasaccharide bis-

Table 1
Initial drop and reservoir concentrations for vapor-diffusion hanging-drop crystallization of unliganded and liganded antigen-binding fragments.

Crystal	Drop	Reservoir
S25-2 Fab unliganded	15 mg ml^{-1} Fab, 0.13 *M* ZnOAc, 13%(*w*/*v*) PEG 8000, 50 m*M* Na cacododylate pH 6.5	0.26 *M* ZnOAc, 25%(*w*/*v*) PEG 8000, 0.1 *M* Na cacodylate pH 6.5
S25-2 Fab–carbohydrate complex	8 mg ml^{-1} Fab with disaccharide antigen, 0.1 *M* ZnOAc, 10%(*w*/*v*) PEG 4000, 0.1 *M* Tris pH 8.5	0.2 *M* ZnOAc, 20%(*w*/*v*) PEG 4000, 0.2 *M* Tris pH 8.5
S45-18 Fab unliganded	6–8 mg ml^{-1} Fab, 10%(*w*/*v*) PEG 8000, 25 m*M* K_3PO_4 pH 7.8	20%(*w*/*v*) PEG 8000, 50 m*M* K_3PO_4 pH 7.8
S45-18 Fab–carbohydrate complex	9 mg ml^{-1} Fab with pentasaccharide bisphosphate antigen, 0.13 *M* $MgCl_2$, 13%(*w*/*v*) PEG 4000, 67 m*M* Tris pH 8.5	0.2 *M* $MgCl_2$, 20%(*w*/*v*) PEG 4000, 0.1 *M* Tris pH 8.5

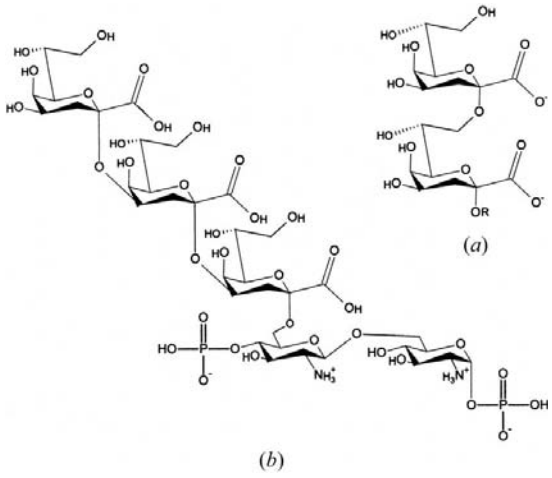

Figure 2
Schematic diagram of carbohydrate antigens used in cocrystallization, present in 40-fold molar excess over Fab. (*a*) The disaccharide α-Kdo-(2,8)-α-Kdo is recognized by S25-2. The 2-OR site represents the location of an allyl substituent in the synthetic derivates that were used in cocrystallization and is also the conjugation site in BSA-glycoconjugates. (*b*) S45-18 was cocrystallized with the pentasaccharide bisphosphate α-Kdo-(2,4)-α-Kdo-(2,4)-α-Kdo-(2,6)-β-GlcN-4P-(1,6)-α-GlcN-1P, containing the specific epitope α-Kdo-(2,4)-α-Kdo-(2,4)-α-Kdo.

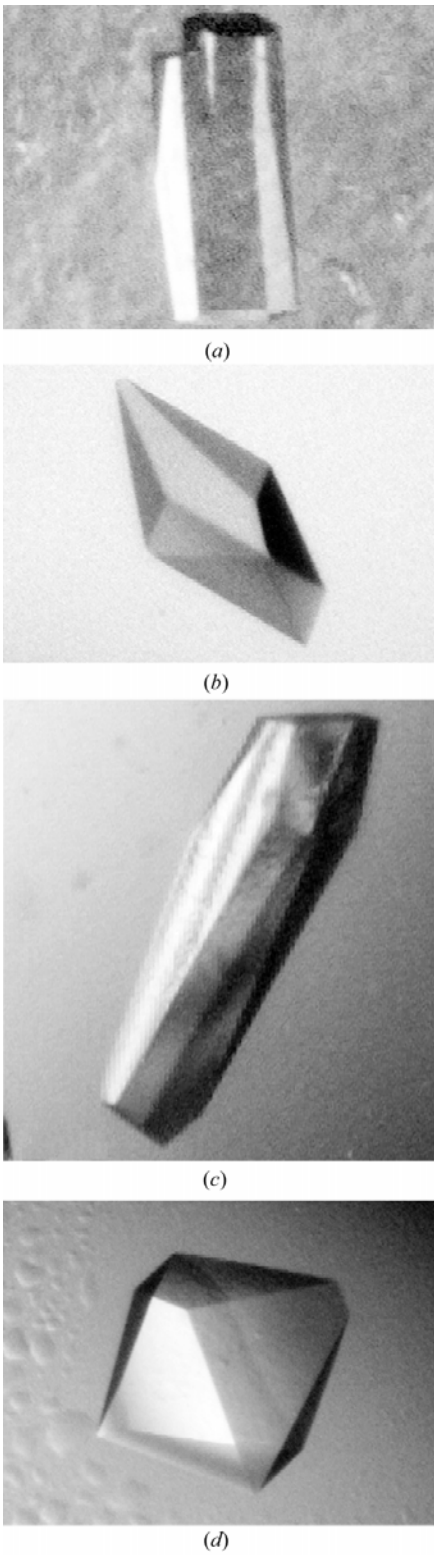

Figure 3
Crystals of (*a*) unliganded S25-2 Fab, (*b*) S25-2 Fab cocrystallized with α-Kdo-(2,8)-α-Kdo disaccharide, (*c*) unliganded S45-18 Fab and (*d*) S45-18 Fab cocrystallized with the pentasaccharide bisphosphate α-Kdo-(2,4)-α-Kdo-(2,4)-α-Kdo-(2,6)-β-GlcN-4P-(1,6)-α-GlcN-1P. For both S25-2 and S45-18, there is a notable improvement in crystal morphology in the presence of antigen.

Table 2
Data-refinement statistics for S45-18 Fab and S25-2 Fab unliganded and cocrystallized with their respective antigens.

Values of reflections in the last resolution shell recorded are presented in parentheses.

	S25-2 Fab unliganded	S25-2 Fab–carbohydrate complex	S45-18 Fab unliganded	S45-18 Fab–carbohydrate complex
Space group	Orthorhombic *I*222	Orthorhombic $P2_12_12_1$	Monoclinic *C*2	Orthorhombic $P2_12_12_1$
Unit-cell parameters (Å, °)	*a* = 70.6, *b* = 97.2, *c* = 136	*a* = 45.9, *b* = 81.6, *c* = 132	*a* = 77.1, *b* = 173, *c* = 77.1, β = 115.0	*a* = 71.2, *b* = 114, *c* = 134
No. molecules per asymmetric unit	1	1	2	2
No. observations	37253	1413166	68816	867920
No. unique reflections	11573	84239	28693	106111
Max. resolution (Å)	3.10	1.43	2.50	1.75
Completeness (%)	85.0 (75.0)	91.4 (57.5)	92.0 (91.5)	95.8 (93.1)
R_{sym}	0.125	0.051 (0.268)	0.098 (0.434)	0.063 (0.396)
$I > 3\sigma(I)$ (%)	60.0 (35.0)	91.0 (78.0)	68.8 (23.9)	76.1 (30.8)

phosphate (Fig. 2) antigens were dissolved in 20 m*M* Tris pH 9.1 and then mixed with the Fab sample (30 mg ml^{-1}) such that the final complex solution contained a 40-fold molar excess of antigen over Fab. S25-2 Fab with α-Kdo-(2,8)-α-Kdo-2-*O*-allyl crystals grew from 6 µl hanging-drops suspended over a 1 ml reservoir. Precipitation was observed in the drop initially and gradually decreased as diamond-face crystals formed within a week in an 291 K incubator. After two weeks (Fig. 3*b*), crystals measuring up to 0.5 × 0.3 × 0.2 mm were frozen. The crystals were removed using rayon loops and briefly dipped into a cryoprotectant solution composed of the reservoir solution with 20% of the water replaced by glycerol, before being transferred to cryo-vials (Hampton Research) filled with liquid-nitrogen-cooled instrument-grade propane (Praxair). S45-18 Fab with α-Kdo-(2,4)-α-Kdo-(2,4)-α-Kdo-(2,6)-β-GlcN-4P-(1,6)-α-GlcN-1P crystals were grown from 6 µl drops over a 1 ml reservoir. Pentagonal face diamond-shaped crystals appeared in the presence of phase separation within a week at room temperature (Fig. 3*d*). After two weeks, crystals with dimensions of up to 0.7 × 0.6 × 0.6 mm were either mounted in glass capillaries for preliminary room-temperature X-ray diffraction collection or frozen using a cryoprotectant solution composed of the reservoir solution with 20% water replaced by glycerol.

2.6. X-ray diffraction data collection

Diffraction and refinement statistics are given in Table 2. Room-temperature X-ray diffraction data was collected using MAR Research model 30 cm and model 345 detectors. Room-temperature unliganded S45-18 Fab crystals diffracted to 2.5 Å resolution. Diffraction data sets from two room-temperature crystals were merged using *DENZO* and *SCALEPACK* (Otwinowski & Minor, 1996). With the S45-18 Fab co-crystallized with antigen, there is a change in space group from monoclinic to orthorhombic. Room-temperature S45-18 Fab–carbohydrate complex crystals diffracted poorly beyond 3.0 Å (data not presented). Diffraction from frozen S45-18 Fab–carbohydrate crystals was collected at the Brookhaven National Synchrotron Light Source, Upton, New York (Area Detector Systems Corporation Quantum 4R CCD detector). Frozen complex crystals scattered visibly to 1.7 Å. Space group and unit-cell values are consistent for the room-temperature and cryocomplex data sets. X-ray diffraction of frozen unliganded S25-2 Fab diffracted poorly beyond 3.0 Å when collected on an ADSC detector at CHESS. Data from frozen S25-2 complex crystals was collected to 1.4 Å, also at NSLS. Preliminary molecular-replacement studies using the program *X-PLOR* (Brünger, 1992) showed strong rotation peaks for each of the four data sets. For S45-18 Fab in both the absence and in the presence of antigen, two molecules per asymmetric unit were found. The calculated V_M (Matthews, 1968) for unliganded S45-18 Fab is 2.41 Å^3 Da^{-1} and for the liganded form is 2.82 Å^3 Da^{-1}. These values suggest solvent contents of 49 and 56%, respectively. For unliganded S25-2 Fab, there is one molecule per asymmetric unit. The V_M is 2.43 Å^3 Da^{-1} and the solvent content is 50%. With S25-2 Fab–carbohydrate complex, there is one molecule per asymmetric unit. The V_M is 2.56 Å^3 Da^{-1}, suggesting a solvent content of 52%.

We are grateful to Dr Z. Jia of the University of Queens, Kingston, Ontario

and Dr D. R. Rose of the University of Toronto, Ontario for allowing us time on their respective area detectors. Acknowledgement is given to the Cornell High-Energy Synchrotron Source and to support members for their assistance. Research carried out (in part) at the National Synchrotron Light Source, Brookhaven National Laboratory is supported by the US Department of Energy, Division of Materials Sciences and Division of Chemical Sciences. We thank J. Berendzen and L. Flaks at NSLS beamline X8C. We also thank M. A. Gidney for propagating the hybridoma cells, H. Tong-Sevinc for assistance with molecular cloning, A. Cunningham for DNA sequence analysis, D. Watson for N-terminal amino-acid sequence analysis and S. Foote for PCR primers.

References

Al-Lazikani, B., Lesk, A. M. & Chothia, C. (1997). *J. Mol. Biol.* **273**, 927–948.

Belunis, C. J., Mdluli, K. E., Raetz, C. R. H. & Nano, F. E. (1992). *J. Biol. Chem.* **267**, 18702–18707.

Borrebaeck, C. A. K. (1992). Editor. *Antibody Engineering: A Practical Guide.* New York: W. H. Freeman & Co.

Brade, H., Brade, L. & Nano, F. E. (1987). *Proc. Natl Acad. Sci. USA*, **84**, 2508–2512.

Brade, L., Kosma, P., Appelmelk, B. J., Paulsen, H. & Brade, H. (1987). *Infect. Immun.* **55**, 462–466.

Brade, L., Rozalski, A., Kosma, P. & Brade, H. (2000). *J. Endotoxin. Res.* **6**, 361–368.

Brünger, A. T. (1992). *X-PLOR Manual, Version* 3.0. Yale University, Connecticut, USA.

Bundle, D. R., Baumann, H., Brisson, J.-R., Gagné, M., Zdanov, A. & Cygler, M. (1994). *Biochemistry*, **33**, 5183–5192.

Capon, S. M. & Goldfinger, D. (1995). *Transfusion*, **35**, 513–520.

Chothia, C., Lesk, A. M., Tramontano, A., Levitt, M., Smith-Gill, S. J., Air, G., Sheriff, S., Padlan, E. A., Davies, D., Tulip, W. R., Colman, P. M., Spinelli, S., Alzari, P. M. & Poljak, R. J. (1989). *Nature (London)*, **342**, 877–883.

Cygler, M., Rose, D. R. & Bundle, D. R. (1991). *Science*, **253**, 442–445.

Duan, L. & Pomerantz, R. J. (1994). *Nucleic Acids Res.* **22**, 5433–5438.

Erlich, H. A. (1989). Editor. *PCR Technology: Principles and Applications for DNA Amplification.* New York: Stockton Press.

Fu, Y., Baumann, M., Kosma, P., Brade, L. & Brade, H. (1992). *Infect. Immun.* **60**, 1314–1321.

Holst, O., Bock, K., Brade, L. & Brade, H. (1995). *Eur. J. Biochem.* **229**, 194–200.

Jeffrey, P. D., Bajorath, J., Chang, C. Y., Yelton, D., Hellström, I., Hellström, K. E. & Sheriff, S. (1995). *Nature Struct. Biol.* **2**, 466–471.

Kabat, E. A. (1988). *J. Immunol.* **141**(Suppl.), S25–S36.

Kalayoglu, M. V., Indrawati, Morrison, R. P., Morrison, S. G., Yuan, Y. & Byrne, G. I. (2000). *J. Infect. Dis.* **181**(Suppl. 3), S483–S489.

Kosma, P. (1999). *Biochim. Biophys. Acta*, **1455**, 387–402.

Matthews, B. W. (1968). *J. Mol. Biol.* **33**, 491–497.

Müller-Loennies, S., MacKenzie, C. R., Patenaude, S. I., Evans, S. V., Kosma, P., Brade, H., Brade, L. & Narang, S. (2000). *Glycobiology*, **10**, 121–130.

Otwinowski, Z. & Minor, W. (1996). *Methods Enzymol.* **276**, 307–326.

Ryan, K. J. (1994). Editor. *Sherris Medical Microbiology.* Toronto: Prentice Hall.

Sambrook, J., Fritsch, E. F. & Maniatis, T. (1989). *Molecular Cloning: A Laboratory Manual*, 2nd ed. Cold Spring Harbor, NY, USA: Cold Spring Harbor Laboratory Press.

Villeneuve, S., Souchon, H., Riottot, M. M., Mazie, J. C., Lei, P., Glaudemans, C. P., Kovac, P., Fournier, J. M. & Alzari, P. M. (2000). *Proc. Natl Acad. Sci. USA*, **97**, 8433–8438.

Zdanov, A., Li, Y., Bundle, D. R., Deng, S. J., MacKenzie, C. R., Narang, S. A., Young, N. M. & Cygler, M. (1994). *Proc. Natl Acad. Sci. USA*, **91**, 6423–6427.